

APPLICATION OF MACROLAMINATION TECHNOLOGY TO LEAN, PREMIX COMBUSTION

Adel Mansour
Parker Hannifin Corporation
Gas Turbine Fuel Systems Division
Mentor, OH, 44060

Douglas L. Straub
U.S. Department of Energy
National Energy Technology Lab
Morgantown, WV

Michael Benjamin
Parker Hannifin Corporation
Gas Turbine Fuel Systems Division
Mentor, OH, 44060

Geo. A. Richards
U.S. Department of Energy
National Energy Technology Lab
Morgantown, WV

ABSTRACT

Macrolamination, a novel manufacturing technique, is used to develop a dual-fuel premixer. A spatially distributed injection strategy is used to enhance fuel placement, distribution, and mixing inside the premixer. Parametric studies are conducted with different configurations of the premixer to determine the effects of residence time and nozzle configuration on pollutant emissions and flame stability. Diesel fuel (DF-2) and natural gas are used as fuels. Tests are conducted at a pressure of 400 kPa (5 atmospheres), and an inlet-air temperature of 533°K. The pollutant emissions and RMS pressure levels are presented for a relatively wide range of nozzle velocities (50-80 m/s) and equivalence ratios (0.54-0.75). These results indicate very good pollutant emissions for a prototype design. These results also indicate that the time-lag model, previously associated with combustion oscillations for gaseous-fuel applications, also applies to liquid-fuel operation.

INTRODUCTION

The power generation industry is faced with increasingly stringent emissions requirements for ozone precursors, such as nitrogen oxides and carbon monoxide. To achieve lower pollutant emissions, gas turbine manufacturers have adopted lean premixed (LP) combustion as a standard technique, particularly for natural gas applications. LP combustion achieves low levels of pollutant emissions without additional hardware for steam injection or selective catalytic reduction (SCR). By premixing the fuel and air, localized regions of near stoichiometric fuel-air mixtures are avoided and a subsequent reduction in thermal NOx can be realized (Appleton and Heywood, 1972; and Lyons, 1982).

Lean premixed combustors for both liquid and gaseous-fuel applications must meet a number of design constraints, including low pressure drop, minimum size, and resistance to flashback. Operating experience has shown that both static and dynamic combustion instabilities are possible and need to be addressed. Static instabilities occur when operational upsets, or changes in fuel properties, produce

unexpected changes in flame anchoring (e.g., flashback, flame extinction near the lean limit, etc.). Dynamic instabilities occur when minor variations in the fuel-air ratio, or mixing processes, lead to significant changes in the combustor heat-release rate. Subsequent coupling between the heat-release rate and the acoustic processes in the combustor can result in large pressure oscillations that can damage mechanical components in the turbine.

In addition to the general constraints outlined above, dual-fuel premixers must be capable of handling different fuels without affecting combustor operability. Additional issues such as autoignition, vaporization, and mixing must be addressed in the design of a dual-fuel premixer. For many years, the importance of LP combustion for dual-fuel applications has been well recognized (Cowell, et al., 1996; Smith and Cowell, 1989; McVey and Kennedy, 1980; and Snyder, et al., 1994). This paper describes test results from a prototype, dual-fuel, premixer designed by Parker Hannifin. Experimental test data are presented that demonstrate the preliminary performance of this premixer in terms of both the measured pollutant emission levels and the RMS pressure levels.

BACKGROUND

To achieve lower levels of NOx emissions, homogeneous fuel-air mixture distributions are necessary. Relative to single-point fuel injection, multi-point fuel injection offers numerous advantages, such as significantly shorter mixing length and time scales. These shorter mixing scales can result in shorter premixer lengths and a significantly lower propensity for flashback and autoignition. Macrolamination is a novel manufacturing technique that allows complex internal flow channels to be formed by fabricating the fuel injectors in layers. The fuel delivery channel, the spin slots, and the swirl chamber are chemically etched into a substrate. Using this macrolamination technology (US Patent 5435884), multi-point fuel injection can be achieved without the associated hardware complexities of conventional designs. Therefore, macrolamination technology is an ideal fit for fabrication and design of

dual-fuel premixers for LP combustion applications. The dual-fuel pre-mixer developed by Parker Hannifin Corporation has been tested at the National Energy Technology Laboratory as part of a Co-operative Research and Development Agreement (CRADA).

The dynamic stability of a dual-fuel pre-mixer is also of interest for gas turbine applications. As previously mentioned, dynamic instabilities can occur when temporal fluctuations in the heat-release rate couple with the resonant acoustics in the combustor. When this type of thermo-acoustic instability occurs, large oscillations in the pressure can occur. These pressure oscillations can have amplitudes on the order of ten percent of the mean combustor pressure and frequencies approaching the kilohertz range. Clearly, this type of cyclic loading can be detrimental to components in a gas turbine.

One of the variables investigated in this study is the fuel-transport time, or residence time, in the pre-mixer. The fuel-transport time, τ , plays a critical role in the phase between the combustor pressure, $P(t)$, and any subsequent variation in the heat-release rate, $Q(t+\tau)$. A number of recent studies (Richards and Janus, 1998; Straub and Richards, 1998; and Liuwen and Zinn, 1998) show the value of altering these time scales to solve dynamics problems. These papers show both experimentally and theoretically how fuel-transport time scales can be changed to produce stable combustion. This idea, however, is not new. Putnam (1971) has shown that by gathering data as a function of flow rate, it is possible to map the stable and oscillating regions in a given combustor. These plots can be generated by plotting the observed RMS pressure levels against the product of the fuel-transport time, τ , and the frequency, f , of the pressure oscillations. This time-lag model suggests that the combustion oscillations are confined to a fairly narrow range of $\tau \cdot f$. This approach of correlating combustion oscillations for a given combustor is widely accepted for natural gas applications. However, for liquid-fuel applications, it is not clear whether this simple time-lag model applies for lean, premixed, pre-vaporized combustors.

In this paper, the prototype dual-fuel pre-mixer is described, as well as the experimental combustor. In the results section, the qualitative effects of residence time, nozzle configuration, and equivalence ratio on the performance of the pre-mixer are discussed. The effects of these variables on NO_x and CO emissions are reported. The RMS pressure levels are also reported at each operating condition. In addition to conducting an evaluation of this prototype design, the validity of using a simple time-lag model to correlate combustion instabilities for liquid-fuel combustion is described.

DESCRIPTION OF EXPERIMENTAL APPARATUS

Premixer Layout

Figure 1 shows a cross-section of the pre-mixer. The liquid-fuel is injected via eight macrolaminate injection tips (see Fig. 1). These injection tips produce fine hollow-cone fuel sprays. Gaseous-fuel injection is achieved through eight radial spokes located between each of the macrolaminate injection tips (see Fig. 1). Each of these radial spokes contains five holes through which gaseous-fuel is injected along the axis of the pre-mixer.

The airflow to the pre-mixer is introduced through a number of different paths. These flow paths are described in the following paragraphs:

Air is admitted axially, along the centerline of the pre-mixer, through several injection holes in the upstream end of the pre-mixer (see Fig. 1; flow path 1). In addition to preventing large-scale recirculation

zones, this axial flow entrains the fuel droplets and directs them toward the centerline. This entrainment process reduces droplet deposition at the wall.

Eight annular air passages surround the macrolaminate injection tips (see Fig. 1, flow path 2). These air jets have the effect of propelling the fuel spray in the axial direction. The additional momentum from these air jets forces the fuel-air mixture to penetrate the swirling air introduced further downstream.

Air is also injected axially along the wall of the pre-mixer (see Fig. 1, flow path 3). This curtain of air surrounds the fuel injectors and acts as an aerodynamic barrier to minimize droplet impingement on the walls. This wall jet also injects sufficient energy into the boundary layer to delay separation.

Two radial-inflow swirlers are positioned to provide sufficient swirl for flame stabilization, and yet minimize the impingement of fuel-droplets on the pre-mixer wall. The initial swirl strength, or swirl number, is maintained relatively low to minimize droplet impingement on the walls. The second swirler adds sufficient swirl to stabilize the flame. The droplet sizes reaching the second swirler are significantly smaller because of vaporization. Therefore, staging the swirl-vane assemblies in this manner is expected to minimize fuel-droplet impingement on the pre-mixer wall, while maintaining sufficient swirl to stabilize the flame.

Experimental Combustor

Many of the details of this combustor have been described previously (Richards and Janus, 1998; Straub and Richards, 1998; and Straub and Richards, 1999). Therefore, only the changes and pertinent details are described here. A cross-section of the experimental combustor is shown in Fig. 2. This combustor is designed specifically to study combustion dynamics, so the hard acoustic boundaries and lack of cooling air passages result in very strong acoustic feedback. It is important to note that this apparatus provides a rigorous test environment for premixers, and the observed RMS pressure levels may not be representative of pre-mixer performance in a realistic gas turbine application. Acoustic losses and rig-to-engine differences in dynamic stability are not well understood.

A cylindrical plug forms the exhaust neck region (see Fig. 2). This plug is fabricated using refractory for the purposes of these tests. Only the material is different from the design described in Straub and Richards (1999). The dimensions and location of this plug are the same as that described in earlier work. An important difference between the results reported in this paper and those reported for previous work, is the location of the water spray that quenches the exhaust gases. In previous work, this water spray has been located immediately downstream of the exhaust neck. To minimize the potential for quenching unburned hydrocarbons or soot, the water quench has been moved approximately 3.8 meters downstream and the vessel length has been increased by 3.6 meters.

Roughly 10 cm downstream of the refractory insert, gas samples are extracted through a stainless steel water-cooled probe. The gas sample is extracted from three locations across the diameter of the exhaust neck region (see Fig. 2). Depending on the flow rate and the gas temperature, the bulk residence time from the inlet of the exhaust neck region to the stainless steel sample probe is 10-20ms. The temperature of the gases exiting the sample probe is about 420°K (300°F). The gas sample then passes through a heated stainless steel line before being cooled in an ice bath to condense the water vapor. The dry gas sample is analyzed for concentrations of NO_x , CO, unburned hydrocarbons, CO_2 , and O_2 at each operating point. In this

paper, only the NO_x and CO emissions will be reported. However, it should be noted that the measured levels of unburned hydrocarbons are negligible for the range of operating conditions investigated.

A natural gas pilot is introduced into the corner region of the combustor through the upstream wall of the combustor liner (see Fig. 2). Pilot fuel is used for startup purposes only. None of the cases reported in this paper utilize pilot fuel to assist the main flame. The intent for operating in this mode is to eliminate the influence of the pilot fuel on the combustion oscillations.

The combustor pressure is maintained with a back-pressure control valve, and the flow in the exhaust neck region is not choked. This design allows operation over a wide range of nozzle velocities at a constant combustor pressure. The inlet-air temperature is controlled using a non-vitiated air preheater, and is also independent of the combustor operating pressure. Therefore, the inlet-air temperature, air-flow rate, and combustor operating pressure can be selected arbitrarily, if necessary. The combustor operating pressure is set at 400 kPa (5 atm.), and allows the rig to operate over a wide range of air and fuel flows, while maintaining a low fuel consumption rate.

The Type-2 diesel fuel used in these tests is a research grade 0.05-percent sulfur fuel. This fuel is chosen to minimize the variability in fuel properties and any subsequent effects on the data. The properties of this fuel are listed in Table 1. The nitrogen content in the fuel is 80 ppm, as measured by an independent laboratory. The contribution of this fuel-bound nitrogen to the measured NO_x emissions is estimated to be less than 5 ppm at 15% oxygen. It should be noted that this is approximately twenty percent of the measured NO_x levels for the best nozzle configuration tested.

Table 1: Diesel Fuel Properties

Carbon (wt%)	86.6
Hydrogen (wt%)	13.4%
Nitrogen	80 ppmw
Specific Gravity (60/60)	.843
API Gravity	36.28
50% Boiling Point	533°K

Instrumentation

The oscillating combustor pressure is monitored using a fast response Kistler (Model 206) pressure transducer. The pressure transducer is installed in an infinite coil to minimize the effects of reflections; similar to the technique described in Mahan and Karchmer (1991). The root-mean square (RMS) value of this dynamic pressure signal is recorded at each operating condition, along with the dominant frequency in the pressure signal. The strength of the combustor oscillations is expressed as a percentage of the mean combustor pressure.

NO_x levels are measured using a Horiba (Model CLA-510SS) chemiluminescent analyzer. CO measurements are taken from a non-dispersive infrared analyzer manufactured by Advanced Pollution Instrumentation Inc. (Model 300). All emissions are reported on a dry basis and have been corrected to 15% O₂.

TEST CONDITIONS

The prototype premixer is a modular design that incorporates different swirl-vanes and spacers. By changing components in the premixer nozzle, the effects of these different nozzle features are investigated. Table 2 shows the nozzle configurations that are discussed in this paper. The overall length of the premixer is constant for the tests reported. The effect of the swirl-vane size and the effect of the downstream swirl-vane are investigated. The swirl-vane thickness (i.e., the number listed in Table 2) refers to the width of the swirl-vane at the outside diameter of the premixer. All of the swirl-vane assemblies have the same outside diameter, and the larger vane sizes correspond to smaller flow areas. Therefore, Case C has the largest flow area of the swirl-vanes tested.

Both the operating pressure and the inlet-air temperature are fixed at 400kPa (5 atm.) and 533°K, respectively. Although the test rig is capable of higher pressures and inlet-air temperatures, these operating conditions are selected to allow testing over a wide range of reference velocities and to conserve fuel.

Besides the geometric premixer configuration, the air flow and the equivalence ratio are also varied. Clearly, increasing the air flow decreases the residence time, but it should also be noted that the nozzle configuration also dramatically alters the fuel residence time. Since the fuel is injected from the base of the premixer, any changes to the nozzle length, or air splits (see Table 3) result in changes to the residence time.

Table 2: Premixer configurations tested. Swirler 2 designates the downstream swirl-vane assembly. Swirler 2 is replaced with a solid-spacer for Case B and Case C.

	Premixer Length (cm)	Vane Thickness Swirler 1 (cm)	Vane Thickness Swirler 2 (cm)
Case A	14.7	0.51	0.51
Case B	14.7	0.51	N/A
Case C	14.7	0.38	N/A

Table 3: The effect of nozzle configuration on the relative air splits

	Approximate Air Split Ratios				
	Y ₁			Y ₂	Y ₃
	Fuel Tip Shroud	Annular Wall Jet	Center-Line Air	Swirler 1	Swirler 2
Case A	0.11	0.13	0.10	0.33	0.33
Case B	0.16	0.20	0.14	0.50	0.00
Case C	0.15	0.17	0.12	0.56	0.00

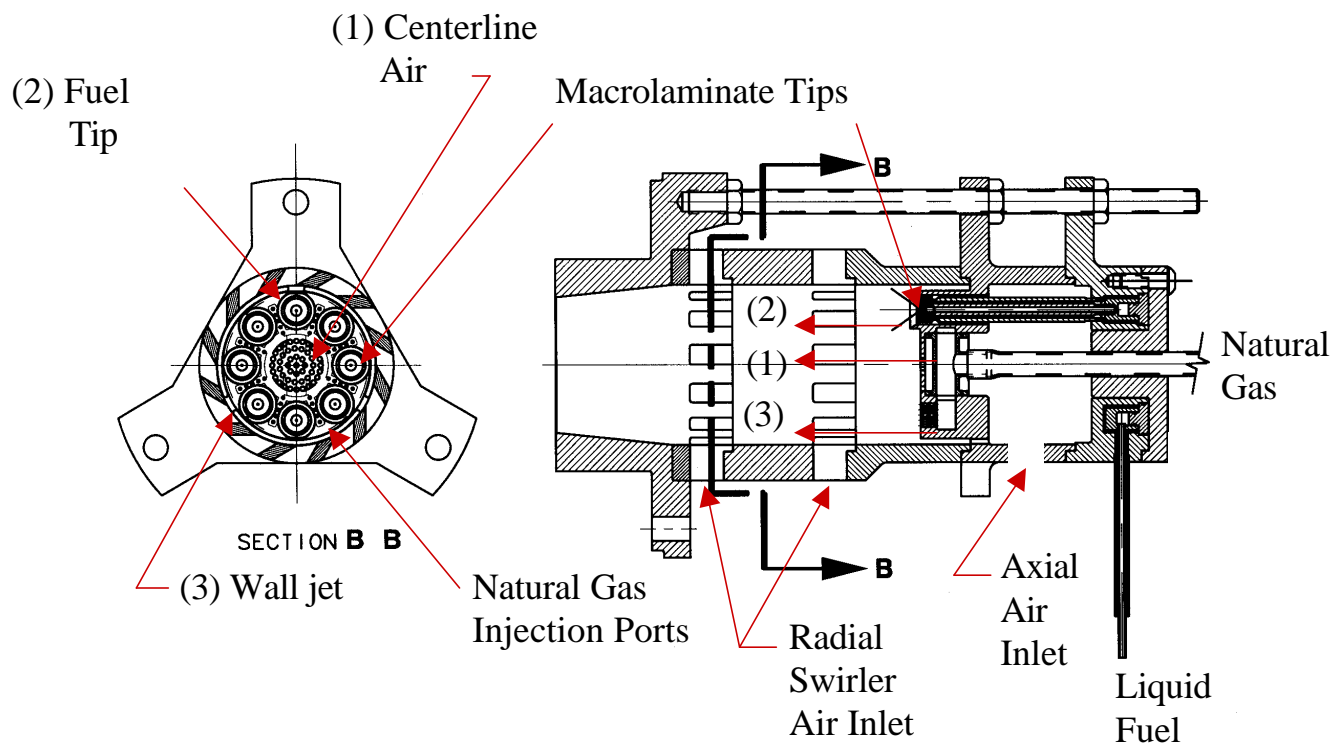


Figure 1: Cross-section of Parker-Hannifin premixer

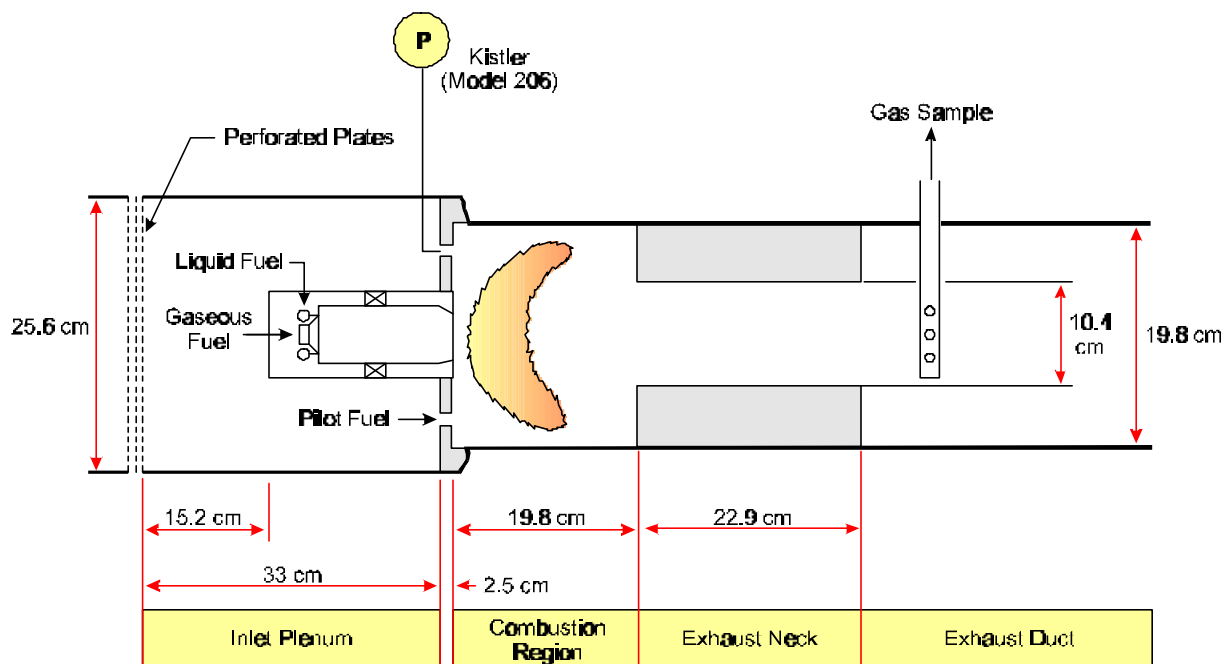


Figure 2: Schematic of experimental FETC combustor

The fuel-transport time is approximated as a function of the average air velocity at the premixer exit, the critical nozzle dimensions, and the approximate air splits for the different configurations. This simplified approach is illustrated in Fig. 3. The fuel-transport time is estimated as

$$t = t_1 + t_2 + t_3 \quad (1)$$

Therefore, the fuel-transport time is simply a sum of the bulk transport times between air injection points along the nozzle axis. The time required to transport a parcel of fuel-air mixture between the fuel-injection plane and the first swirler is denoted as τ_1 . Similarly, τ_2 is the time required to advect the parcel of fuel-air mixture between the first swirler and the second swirler; and τ_3 is the time required to advect the parcel of fuel-air mixture between the second swirler and the exit of the premixer (see Fig. 3). Therefore, the bulk fuel-transport time can be approximated using the nozzle configuration and approximate air splits as shown in Equation 2. The reader should refer to Fig. 3 for the definition of the various parameters and Table 2 for the approximate air splits for each of the nozzle configurations tested

$$t = \left(\frac{L_1 - L_2}{y_1 U} \right) + \left(\frac{L_2 - L_3}{(y_1 + y_2) U} \right) + \left(\frac{L_3}{U} \right) \quad (2)$$

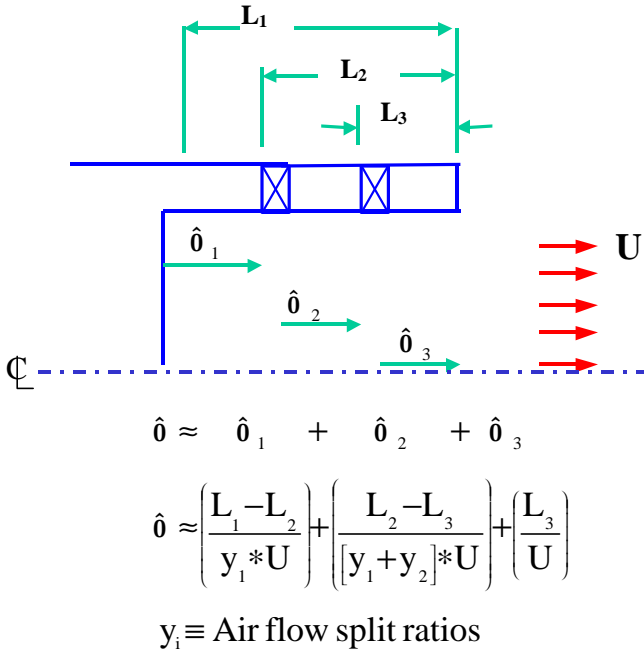
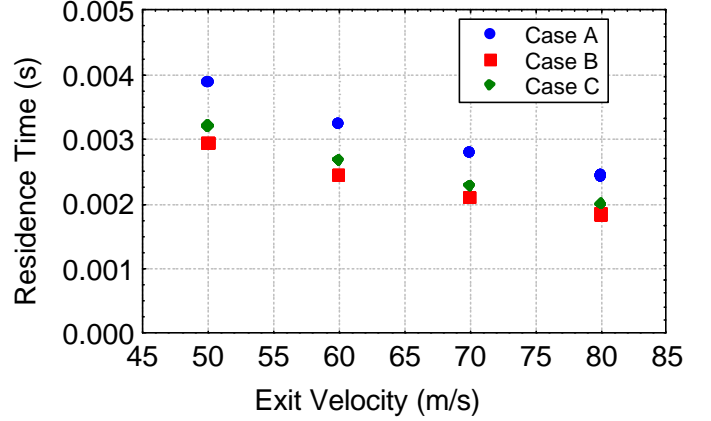


Figure 3: Approach to calculate fuel residence time

Equation 2 shows that the fuel-transport time, τ , is equal to the length of the section divided by the average, or bulk air velocity. The velocity, U , is calculated based on the measured air flows and exit area of the nozzle. This velocity represents the average (plug flow) value at the nozzle exit. Obviously, this approximation does not consider the details of the flow field inside the premixer. Each

individual section would see a range of transport times that are distributed around the average transport time approximated by Eq.2. Nonetheless, the notion of an average transport time is very useful for engineering purposes. Figure 4 shows the range of transport times



obtained using the above equation for all three cases discussed in this paper as a function of average exit velocities. Note that Case A has the longest transport time, and Case B has the shortest transport time.

Figure 4: Range of fuel transport times

RESULTS

The overall NO_x and CO emission data for DF-2 are shown in Fig. 5. It should be noted that each point shown in Fig. 5 represents a specific equivalence ratio and air-flow rate that is replicated for each premixer configuration, so an equal number of points are shown for each nozzle configuration. Although all of the configurations produced CO emissions below 15 ppm, Case B exhibited the lowest NO_x levels. Furthermore, Case B produced lower levels of NO_x over a wider range of operating conditions. Therefore, the configuration in Case B produces the best pollutant emission performance for the range of operating conditions investigated.

Although Fig. 5 shows both the NO_x and CO levels, additional information is obtained by looking at the NO_x emissions as a function of the adiabatic flame temperature (see Fig. 6). The adiabatic flame temperature is calculated by the procedure outlined by Gulder, 1986. These calculated temperatures agree to within one percent of values from chemical equilibrium codes. The data in Fig. 6 show that the NO_x levels vary significantly depending on the operating condition.

Consider the data from Case A on liquid-fuel at a nozzle exit velocity of 80 m/s. As the equivalence ratio, or adiabatic flame temperature, is decreased, the NO_x emissions decrease until the adiabatic flame temperature approaches 1950°K. When the adiabatic flame temperature is decreased below 1950°K, the NO_x emissions actually increase. This behavior is repeatable to within about 3 ppm on the NO_x measurements. However, hysteresis is observed, so the actual flame temperature at which this transition occurs depends on whether this transition is approached from a lower flame temperature or a higher flame temperature. The data shown in this paper are collected as the flame temperature is decreased. As Fig. 6 shows, this behavior is not observed for all the premixer configurations.

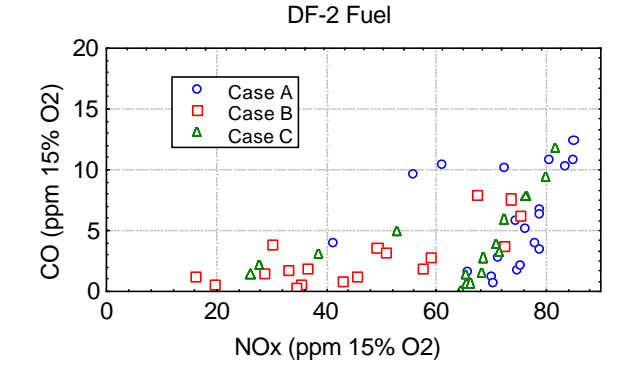


Figure 5: Pollutant emissions for all nozzle configurations and all operating conditions ($50 < U < 80$ m/s, $0.55 < N < 0.75$, 5 atm, 533°K)

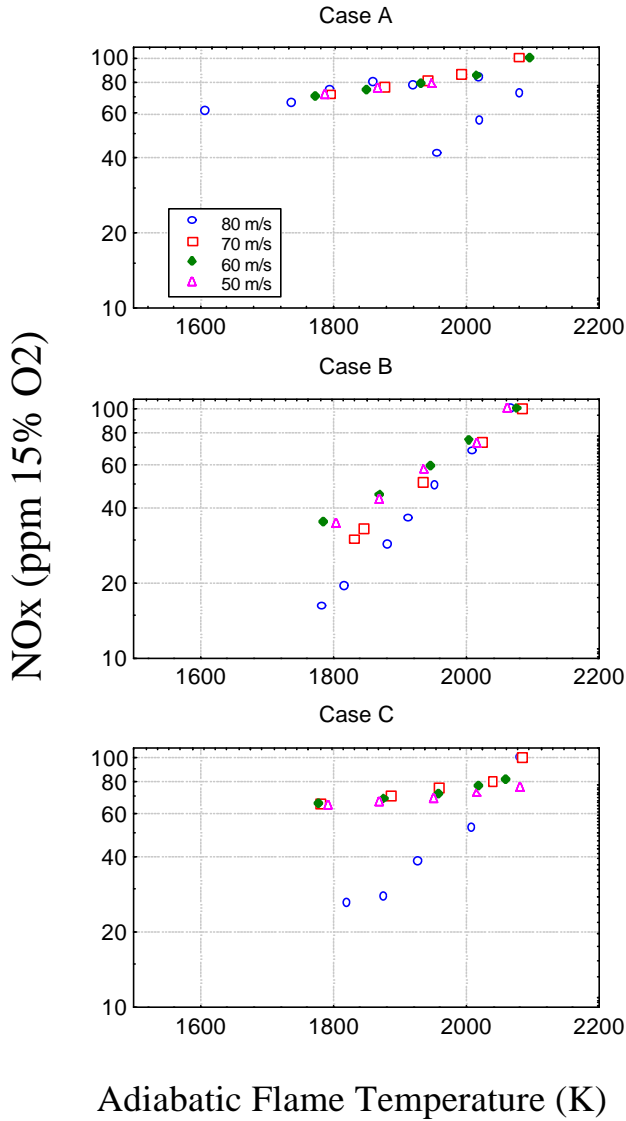


Figure 6: NOx emissions as a function of nozzle configuration and adiabatic flame temperature (DF-2 fuel). No pilot fuel is used, so leaner conditions are not investigated

The RMS pressure levels show the same “on-off” transition. Figure 7 shows both the NOx emissions (thin line) and the RMS pressure levels (thick line) as a function of equivalence ratio for Case A (DF-2 fuel and a velocity of 80 m/s). As the NOx emissions increase, the RMS pressure levels decrease sharply for values of equivalence ratio below 0.62. It is believed this behavior is caused by a change in the flame location. When the RMS pressure levels are low, the flame zone is believed to be located closer to the premixer tip. The change in flame location is confirmed by a thermocouple added to the wall of the premixer. This thermocouple registers temperatures above 533°K when the RMS pressure levels are low. When the RMS pressure levels are high (greater than 0.5 percent) and the NOx levels are relatively low, the thermocouple reading is considerably lower. It is believed that the change in flame location produces a diffusion-type flame that results in higher NOx emissions and lower RMS pressure levels. When the RMS pressure levels are high, the flame is likely burning in a premixed mode and the NOx emission levels are reasonably lower.

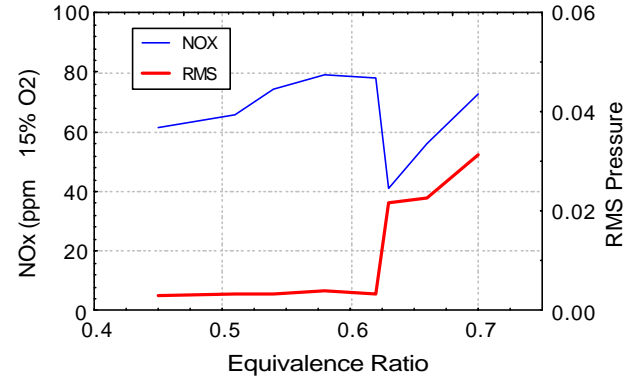


Figure 7: NOx/RMS pressure level relationship (Case A, 80 m/s, DF-2 fuel).

Figure 8 shows the RMS pressure levels for all three cases studied (both natural gas and DF-2). Note that the RMS pressure levels for the liquid-fuel cases are extremely low (less than 0.5 percent) for many of the operating conditions investigated. At these low values of the RMS pressure, it is believed that the flame anchoring location has changed. Although the level of the combustion oscillations for Case B is higher, the measured NOx concentrations are lower.

Figure 9 shows the RMS pressure levels for all of the operating conditions investigated. These RMS pressure levels are plotted against the product of the fuel time-lag, τ , and the dominant frequency, f , in the pressure signal. The fuel time-lag is approximated by Eq. 2. However, to account for the additional time lag between the tip of the premixer and the location of the flame zone, a constant flame-standoff distance of 2.54 cm is assumed for all operating conditions. Therefore, the time-lag values presented in Fig. 9 represent the sum of the fuel residence time in the nozzle (Eq. 2) and an approximate time lag between the nozzle exit and the flame front. This approach is identical to the approach used in previous work. Figure 9 shows that despite a factor-of-two change in the fuel-transport time, these results are correlated by a simple time-lag approach. In fact, the range of time-lag values over which large RMS pressure levels are observed is consistent with

previous results from different premixers tested in this rig (Straub and Richards, 1998).

The liquid-fuel results also obey a time-lag model, as shown in Fig. 9. However, the bands appear to be considerably narrower than for natural gas, and a second band of data is observed around a τ^*f product of 0.8. These results differ from the natural gas operating experience that shows the region between τ^*f values of 0.7 to 1.1 are generally dynamically stable. Although these variations are not well understood, these differences may be explained by the inherent assumptions used in calculating the fuel-transport time. Perhaps small changes in the flame location, or shape, for the natural gas results can alter the actual fuel time-lag enough to cause the combustor to oscillate in a different τ^*f band. When calculating the fuel-transport time, assumptions are made about the flame location and shape. Perhaps a better measurement of fuel-transport time is warranted. In fact, the flame location and shape may play a much more critical role in determining the dynamic stability of the combustor.

To further investigate whether the DF-2 fuel data conforms to the behavior of a simple time-lag model, the frequency of the combustor oscillation is plotted as a function of the reference velocity (see Fig. 10). As explained in Straub and Richards (1998), the oscillating frequency will cover a range of values near the natural frequencies of the combustor. According to the time-lag description, if the velocity decreases (fuel time-lag increases), the frequency of the oscillation will decrease to maintain a constant τ^*f product. If the frequency is sufficiently far from the natural frequency or the acoustic losses exceed the magnitude of the combustion driving term, the combustion will be stable. Figure 10 shows that the frequency decreases with velocity, as predicted by a simple time-lag model. Figure 10 shows how the air flow, or velocity, through the nozzle can be altered to control the τ^*f product.

Figure 7 NOx/RMS pressure level relationship (Case A, 80 m/s, DF-2 fuel)

Consider the data shown in Fig. 10. At 80 m/s, both operating conditions produced combustion oscillations (see Fig. 8, Case B, DF-2 Fuel), and the observed values of the τ^*f product are within the unstable range (0.37-0.43) shown in Fig. 9 for DF-2 fuel. By reducing the nozzle reference velocity from 80 m/s, τ increases and the time-lag model predicts that the frequency must decrease to maintain a constant τ^*f product. At 70 m/s, Fig. 10 shows that the lean operating point is near the edge of the unstable range for the τ^*f product, and the frequency for the richer operating point has shifted to a lower value which puts it in the stable range. Indeed, the leaner condition is unstable and the richer condition is stable, as shown in Fig. 8. As the velocity is reduced further, the frequencies for both operating conditions transition into the 110-125 Hz frequency band. The acoustic feedback from this lower frequency range is not as strong as the 160-180 Hz band, so even though the time-lag model predicts an unstable phase relation at 50 m/s, the gain at this frequency is not large enough to make the system unstable.

CONCLUSIONS

A prototype lean premixed pre-vaporized fuel nozzle has been designed and successfully tested to demonstrate performance at 533°K inlet-air temperature and 400 kPa (5 atmospheres). After testing a number of nozzle configurations, NOx and CO emissions of less than

20 ppm are observed for both DF-2 and natural gas. These results are encouraging for a prototype dual-fuel premixer. It is important to note that reported results are obtained without any pilot fuel to stabilize the flame.

The observed RMS pressure levels and NOx emissions are very sensitive to changes in flame location. It has been observed that when the RMS pressure levels are significant (i.e., greater than 0.5 percent), the observed NOx levels are relatively low. However, sudden changes in the flame location, as indicated by a thermocouple installed along the wall of the premixer, can lead to significantly higher NOx emissions and lower RMS pressure levels. The transition in the flame location is sensitive to the nozzle configuration and the operating conditions.

A time-lag model can be used to correlate and guide approaches for solving combustion oscillations in liquid, and dual-fuel, applications. An approach to estimate the fuel-transport time in a premixer with multiple air-injection locations has been described. In spite of a factor-of-two variation in the fuel-transport time, the observed combustion oscillations for lean premixed prevaporized liquid-fuel applications can be correlated using a time-lag description, similar to approaches that have been used for gaseous-fuel applications.

REFERENCES

- Appelton, J. P., and Heywood, J. B., "The effects of Imperfect Fuel-Air Mixing in a Burner on NO Formation from Nitrogen in the Air and the Fuel," 14th International Symp. on Combustion, pp. 777-786, 1972;
- Cowell, L. H., A. Rajput, and D. C. Rawlins (1996), "Development of a Dual-Fuel Injection System For Lean Premixed Industrial Gas Turbines," ASME 96-GT-195.
- Gulder, O. L., (1986), "Flame Temperature Estimation of Conventional and Future Jet Fuels," ASME Journal of Engineering for Gas Turbines and Power, Vol 108, pp 376-380.
- Lieuwen, T. and B. T. Zinn (1998), "Theoretical Investigation of Combustion Instability mechanisms in Lean Premixed Gas Turbines," AIAA 98-0641.
- Lyons, V. J., "Fuel/Air Non-uniformity Effects on Nitric Oxide Emissions," AIAA Journal, Vol. 20, pp. 660-665, 1982;
- Mahan, J. R., and A. Karchmer (1991), "Combustion Core Noise," in Aeroacoustics of Flight Vehicles: Theory and Practice, Volume 1: Noise Sources, NASA Langley Research Center, Available from AIAA Technical Library.
- McVey, J. B., and Kennedy, J.B., "Lean Stability Augmentation Study", Journal of Energy, Vol. 4, 1980.
- Putnam, A. A., (1971), Combustion Driven Oscillations in Industry, American Elsevier Publishing, New York, NY.
- Richards, G. A., and M. C. Janus (1998), "Characterization of Oscillations During Premix Gas Turbine Combustion," ASME Journal of Engineering for Gas Turbines and Power, Vol 120, No. 2, pp. 294-302.
- Snyder, S. S., Rosfjord, T. J., McVey, J.B., Chiappetta, L. M., "Comparison of Fuel/Air Mixing and NOx Emissions for Tangential Entry Nozzle, ASME 94-GT-283, 1994.
- Smith, K. O., and Cowell, L.H., "Experimental Evaluation of Liquid-Fueled, Lean-Premixed Gas Turbine Combustor," ASME 89-GT-264, 1989.

Straub, D. L., and G. A. Richards (1998), "Effect of Fuel Nozzle Configuration on Premix Combustion Dynamics," ASME 98-GT-492.

vane Location On Combustion Dynamics," ASME 99-GT-109.

Straub, D. L., and G. A. Richards (1999), "Effect of Axial Swirl-

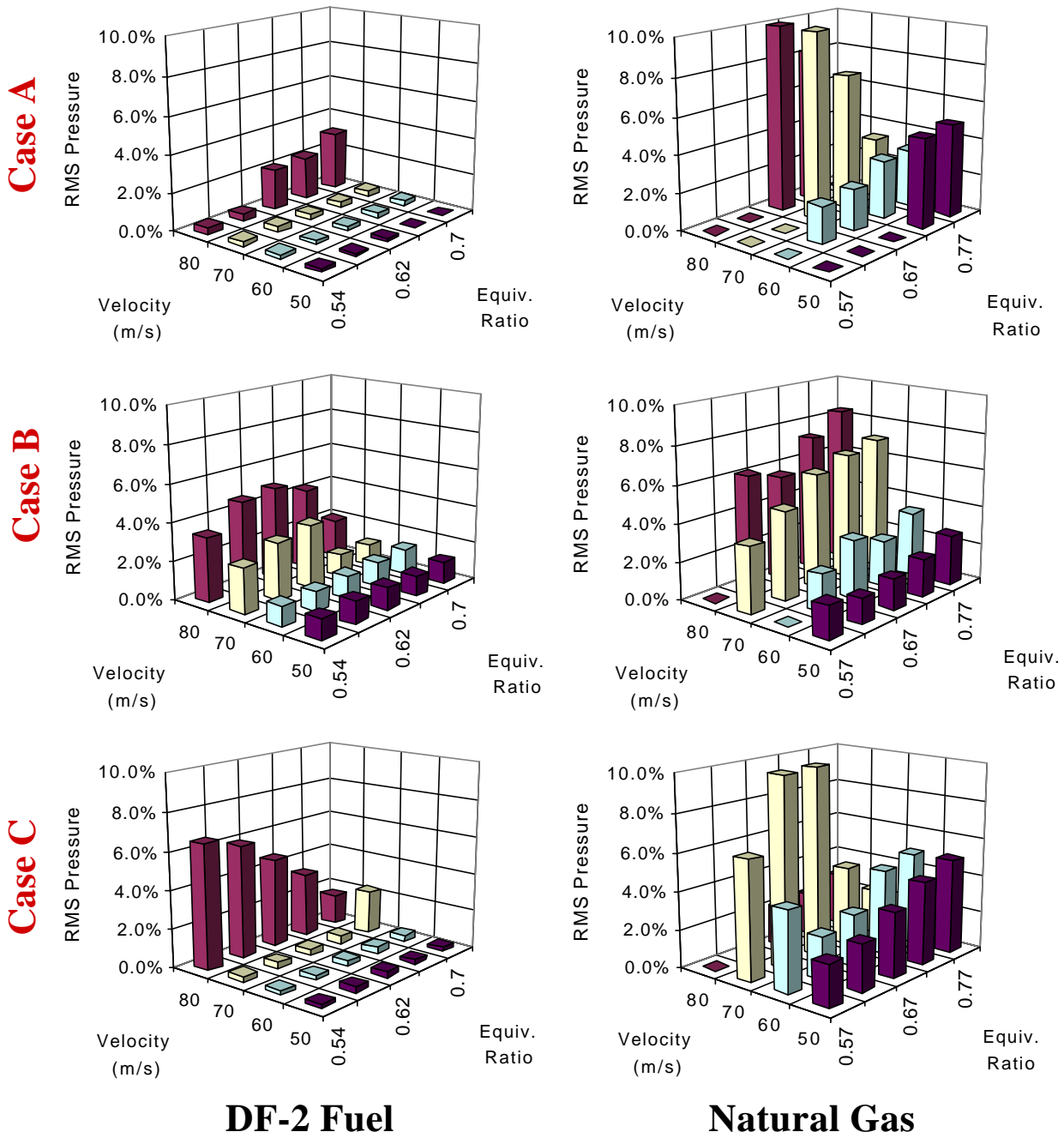


Figure 8: Stability maps for each nozzle configuration and fuel type

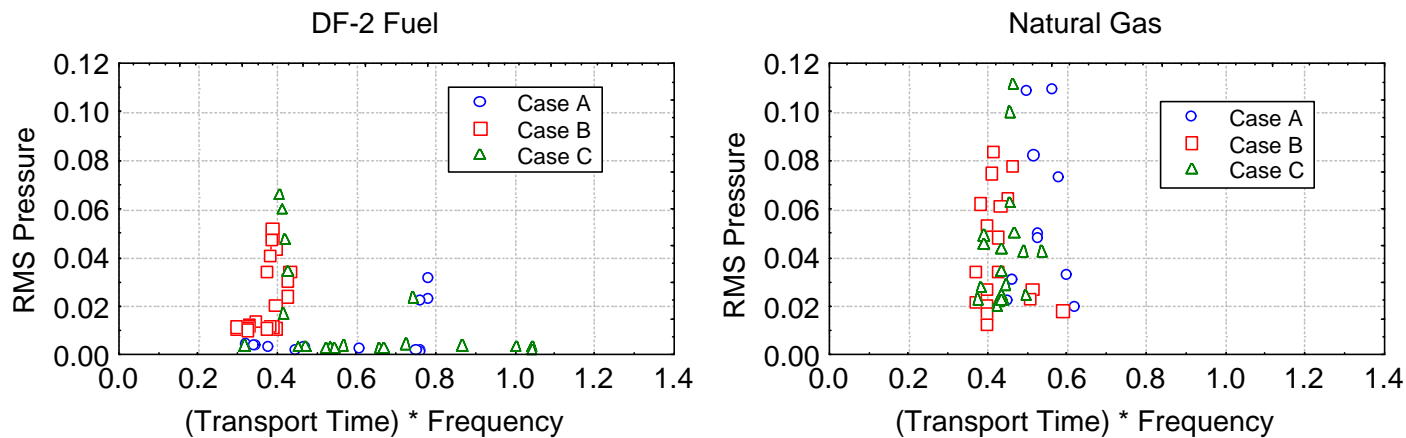


Figure 9: Time lag model description of the experimental results. Both fuel types can be described by a simple time lag.

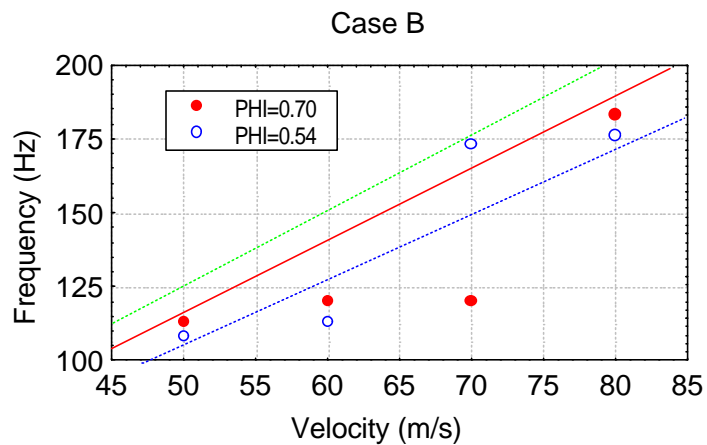


Figure 10: Dominant frequencies observed as a function of velocity for two equivalence ratio conditions (Case B on DF-2 fuel). Constant values of $(\text{transport time}) * \text{frequency}$ are also shown.